ELSEVIER

Biophysical Chemistry 126 (2007) 165–175

Biophysical Chemistry

http://www.elsevier.com/locate/biophyschem

Energetic basis of molecular recognition in a DNA aptamer

G. Reid Bishop [a,*], Jinsong Ren [b], Brandon C. Polander [a], Benjamin D. Jeanfreau [a], John O. Trent [c], Jonathan B. Chaires [c,*]

[a] *Department of Chemistry and Biochemistry, Mississippi College, 200 S. Capitol St., Clinton, MS 39058, USA*

[b] *Key Laboratory of Rare Earth Chemistry and Physics, Changchun Institute of Applied Chemistry, Chinese Academy of Sciences, Changchun, Jilin 130022, China*

[c] *James Graham Brown Cancer Center, Health Sciences Center, University of Louisville, 529 S. Jackson St., Louisville, KY 40202, USA*

Received 31 March 2006; accepted 23 July 2006
Available online 17 August 2006

Abstract

The thermal stability and ligand binding properties of the L-argininamide-binding DNA aptamer (5′–GATCGAAACGTAGCGCCTTCGATC–3′) were studied by spectroscopic and calorimetric methods. Differential calorimetric studies showed that the uncomplexed aptamer melted in a two-state reaction with a melting temperature $T_m = 50.2 \pm 0.2$ °C and a folding enthalpy $\Delta H°_{fold} = -49.0 \pm 2.1$ kcal mol^{-1}. These values agree with values of $T_m = 49.6$ °C and $\Delta H°_{fold} = -51.2$ kcal mol^{-1} predicted for a simple hairpin structure. Melting of the uncomplexed aptamer was dependent upon salt concentration, but independent of strand concentration. The T_m of aptamer melting was found to increase as L-argininamide concentrations increased. Analysis of circular dichroism titration data using a single-site binding model resulted in the determination of a binding free energy $\Delta G°_{bind} = -5.1$ kcal mol^{-1}. Isothermal titration calorimetry studies revealed an exothermic binding reaction with $\Delta H°_{bind} = -8.7$ kcal mol^{-1}. Combination of enthalpy and free energy produce an unfavorable entropy of $-T\Delta S° = +3.6$ kcal mol^{-1}. A molar heat capacity change of -116 cal mol^{-1} K^{-1} was determined from calorimetric measurements at four temperatures over the range of 15–40 °C. Molecular dynamics simulations were used to explore the structures of the unligated and ligated aptamer structures. From the calculated changes in solvent accessible surface areas of these structures a molar heat capacity change of -125 cal mol^{-1} K^{-1} was calculated, a value in excellent agreement with the experimental value. The thermodynamic signature, along with the coupled CD spectral changes, suggest that the binding of L-argininamide to its DNA aptamer is an induced-fit process in which the binding of the ligand is thermodynamically coupled to a conformational ordering of the nucleic acid.

Keywords: DNA; Aptamer; Thermodynamics; Entropy; Enthalpy; Calorimetry; Circular dichroism; Molecular recognition; Induced fit

1. Introduction

Single-stranded DNA and RNA aptamers that selectively bind target amino acids [1–4], nucleotides [5], metal ions, proteins [6,7], and other molecules [8,9] have been identified from random sequence libraries by the SELEX method [10–12]. Since the first report of the SELEX method by the Gold laboratory in 1990 [12], reports of DNA and RNA aptamers have increased in the chemical and patent literature. DNA and RNA aptamers are of interest for three main reasons. First, aptamers are important in biotechnology as novel catalysts and biosensors. Aptamers selectively bind ligands with affinities that rival monoclonal antibodies [13–15]. Second, DNA aptamers may themselves act as potential therapeutics. For example, AS1411 (a derivative of the quadruplex GRO29A [16]) is in clinical trials and has recently been granted orphan drug status for the treatment of renal and pancreatic cancers (see: www.antisoma.com). Finally, aptamers represent interesting model systems for investigating molecular recognition, including the thermodynamic linkage between ligand binding and nucleic acid folding. To date, the majority of the biophysical studies involving DNA aptamers were aimed at structural determinations [17,18]. Very few detailed thermodynamic studies in which the energetics of binding between an aptamer and its cognate ligand have been reported, although there are exceptions [19–21].

* Corresponding authors. J.B. Chaires is to be contacted at tel.: +1 502 852 1172; fax: +1 502 852 1153. G.R. Bishop, is to be contacted at tel.: +1 601 925 7665; fax: +1 601 925 3933.

E-mail addresses: rbishop@mc.edu (G.R. Bishop), jbchai01@gwise.louisville.edu (J.B. Chaires).

0301-4622/$ - see front matter © 2006 Elsevier B.V. All rights reserved.
doi:10.1016/j.bpc.2006.07.009

Here we determine the thermodynamic signature that characterizes the binding of L-argininamide (L-Arm) to its 24 nt DNA aptamer (Fig. 1). The structure of a truncated version of an argininamide–DNA aptamer [1] complex was reported [2], and coordinates were deposited with the PDB accession code 1OLD. For convenience, we will refer to both the ligated and unligated aptamer sequence as 1OLD. 1OLD is one of four known sequences that specifically target arginine-like ligands whose structures have been determined by NMR spectroscopy. Of these four aptamers, three are comprised of DNA [2–4] and one is an RNA sequence that is based on the *trans*-activation response (TAR) sequence of the RNA genome of HIV-2 [22]. The PDB accession codes of the three DNA aptamers are 1OLD [2], 1DB6 [3], and 2ARG [4]. These aptamers contain 24, 22, and 30 nts, respectively, while the RNA aptamer is a 30 nt sequence whose structure is designated as 1AJU [22].

In the case of each of the DNA aptamers, the three-dimensional structure of the nucleic acid is reported to be at least partially disordered in the absence of ligand, with the structure of large regions of the molecule unsolvable by NMR methods [2–4]. In the presence of the ligand L-Arm, however, each of the DNA aptamers becomes more ordered, and accessible to structural characterization by NMR spectroscopy. The structures of 1OLD and the 1AJU RNA structure are each characterized by the coplanar alignment of the guanidinium group of the L-Arg ligand with the Watson–Crick edge of a cytosine base which forms two hydrogen bonds with the ligand [2,22]. In the case of 1OLD, the specific base making the interaction is the C_9 cytosine (Fig. 1C). The binding pocket of 1OLD is flanked by stacked base pairs. The ligand binding pocket of 2ARG the argininamide side chain is positioned between the Hoogsteen face of a coplanar guanine and a tilted cytosine base [4]. Stacking and tilted bases encase the binding pocket in both 2ARG and 1AJU. Thus, in 1OLD, 2ARG, and 1AJU, the guanidinium group is found encapsulated in a binding pocket lined by the hydrogen bonding edges of the bases, maximizing sequence specific molecular interactions. In contrast, the binding of L-Arm to the DNA aptamer 1DB6 [3] is stabilized largely by an electrostatic interaction occurring between the guanidinium group and the phosphate backbone of the DNA aptamer.

The experiments presented in this paper were designed to determine the thermodynamic signature for the binding L-Arm to 1OLD (Fig. 1) in order to test the hypothesis that the binding reaction occurs by an induced-fit binding mode [23]. For an induced-fit mechanism, the thermodynamics of ligand binding ought to reveal an entropically unfavorable contribution that arises from the coupled ordering of the binding site [23–28]. A large, favorable enthalpy is expected and is needed to overwhelm the entropic penalty from ordering the binding site. That is the behavior we observe experimentally and report here for the binding of L-argininamide to its DNA aptamer.

2. Materials and methods

2.1. DNA oligonucleotides and buffers

DNA oligonucleotides were purchased from Oligos Etc. (www.oligosetc.com) and MWG Biotech (www.mwg-biotech.

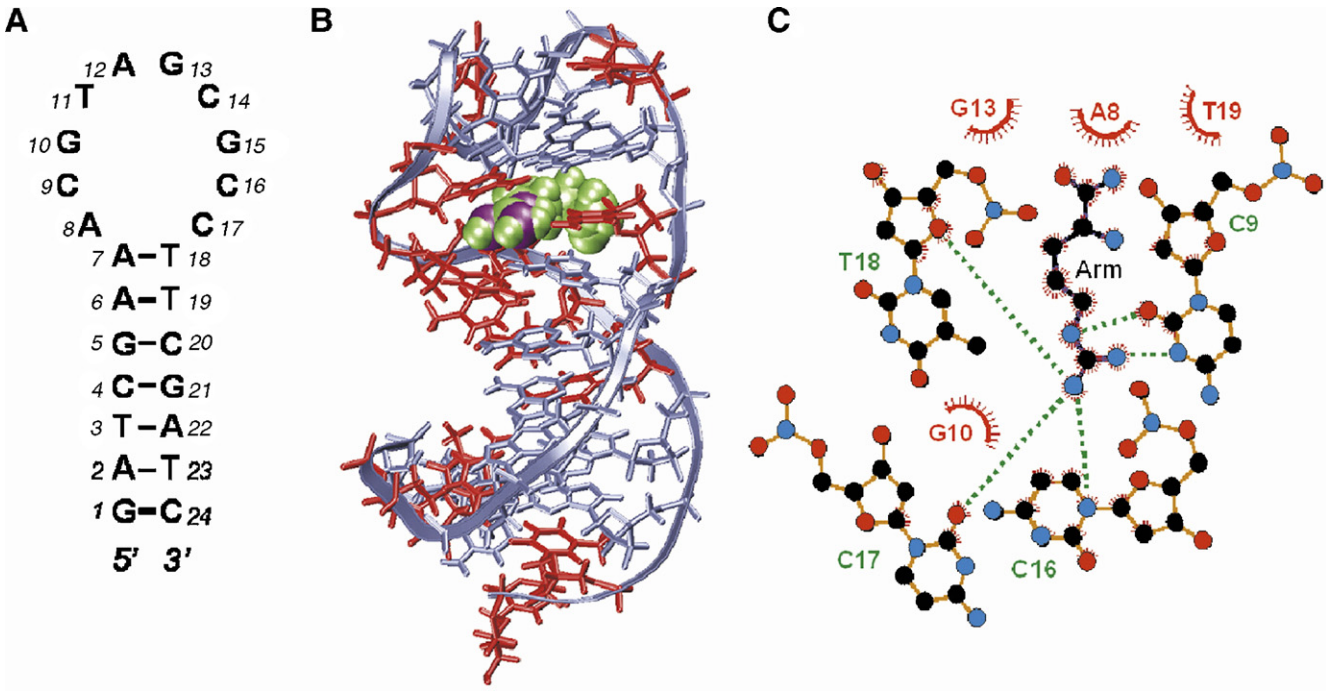

Fig. 1. Structural details of the 1OLD DNA aptamer. (A) The sequence and putative secondary structure of 1OLD in the absence of L-Arm as predicted by the *Mfold* algorithm. (B) The rendering of the 3-dimensional structure of 1OLD obtained from the Protein Data Bank (PDB entry 1OLD). The phosphodiester backbone is shown as a blue colored ribbon. Pyrimidine nucleotide residues are colored blue and purine nucleotide residues are colored red. The ligand L-argininamide (L-Arm) is depicted in green in its space-filling representation. The guanidinium nitrogens of L-Arm are colored purple. (C) The resulting LigPlot of 1OLD as downloaded from the Protein Data Bank's PDB Summary page. (For interpretation of the references to colour in this figure legend, the reader is referred to the web version of this article.)

com) and were used without further purification. Molar extinction coefficients for the single-stranded oligonucleotides were calculated using the standard nearest-neighbor method [29]. All thermodynamic experiments were performed in a buffer composed of 10 mM sodium phosphate, 50 mM KCl, pH 6.5. Additionally, HPLC purified DNA deoxyoligonucleotides were also obtained from MWG Biotech as lyophilized powders for use in the heat capacity determination experiments. L-Argininamide was obtained from Sigma Chemical Co.

2.2. Circular dichroism spectropolarimetry

Circular dichroism spectra were recorded at 20 °C on a Jasco J500A spectropolarimeter (Jasco, Inc., Easton, MD) interfaced to an IBM PC computer [30].

2.3. UV melting experiments

Ultraviolet DNA aptamer melting curves were determined using a Cary 3E UV/Visible Spectrophotometer (Varian, Inc., Palo Alto), equipped with a thermoelectric temperature controller. Samples were heated at a rate of 1 °C min^{-1}, while continuously monitoring the absorbance at 260 nm. Primary data were transferred to the graphics program Origin 6.1 (Microcal, Inc., Northampton, MA) for plotting and analysis.

In addition to the single wavelength melts, three-dimensional melting studies were performed using an Agilent 8453 diode array spectrophotometer with 1 nm resolution and equipped with a programmable thermoelectric temperature controller. In these experiments, whole spectra were collected every 0.5 °C with a 1-min hold time.

2.4. Analysis of optical melting curves by direct fitting

Single-wavelength melts were analyzed by several methods, including direct fits of melting curves [31]. Direct fit of melting curves used a model (Eqs. (1a)–(1f)) that was derived for a single-transition melting transition with corrections for both pre- and post-transition baselines. All single wavelength traces were fit by Eq. (1f) (based on Eqs. (1a)–(1e)) using GraphPad Prism 4.0 and Origin 6.1.

$$A_U = \{b_U + (m_U{*}T)\} \tag{1a}$$

$$A_L = \{b_L + (m_L{*}T)\} \tag{1b}$$

$$\Delta T = \left\{\frac{1}{273.15 + T_m} - \frac{1}{273.15 + T}\right\} \tag{1c}$$

$$Q = \left\{\frac{\Delta H}{8.314472}\right\} \tag{1d}$$

$$r = \left\{\frac{1}{1 + \exp^{(Q{*}\Delta T)}}\right\} \tag{1e}$$

$$A(T) = \{[(1 - r){*}A_U] + [r{*}A_L]\} \tag{1f}$$

In Eq. (1f), $A(T)$ is the dependent variable and is the experimentally determined absorbance at each temperature (T). In Eq. (1a), (1b) and (1f), A_U and A_L are linear equations describing the upper and lower baselines, respectively, where b_U and b_L are fitted parameters for the intercepts for the upper and lower baseline, respectively, and m_U and m_L are the slopes of those same baselines. The fitted value of T_m is taken to be the temperature at which the fraction folded is 50% and ΔH is the enthalpy for the denaturation in joules per mole. All enthalpies were ultimately converted to kcal mol^{-1}. (Note: In Eq. (1a)–(1e), several variables including A_U, A_L, ΔT, Q, and are used in successive equations as placeholders for the mathematical relationships that they represent. Eq. (1f) is the actual fitting function.)

2.5. Analysis of optical melting curves by the fraction folded (α(T))methods

For each of the following analyses, it is first necessary to cast raw optical melting data into the fraction of the aptamers folded at each temperature α(T)) according to the methods outlined in Plum [32]. To accomplish this, upper and lower baselines $A_U(T)$ and $A_L(T)$, respectively, were determined by fitting the linear portions of the absorbance ($A(T)$)versus temperature (T) curve. Next the fraction folded parameter α(T) was computed for each temperature (T) according to Eq. (2).

$$\alpha(T) = \frac{A_U(T) - A(T)}{A_U(T) - A_L(T)} = \frac{m_U T + b_U - A(T)}{(m_U - m_U)T + b_U - b_L} \tag{2}$$

where $A_U(T)=m_U T+b_U$ and $A_L(T)=m_L T+b_L$. Following baseline subtraction the thermodynamic parameters T_m and $\Delta H°$ can be extracted from plots of α(T) versus $1/T$ or T using a variety of methods [32]. Optical melting curves for the DNA aptamer designated as 1OLD were analyzed by each method.

2.6. Monte Carlo analysis of optical melting curves

Optical melt data that were analyzed by non-linear regression were additionally subjected to Monte Carlo methods [33,34] for the determination of the error of fitted parameters T_m, $\Delta H°$, b_U, m_U, b_L, and m_L. In these analyses, the Monte Carlo studies were performed using the built in methods of GraphPad Prism 4.0. In each of three separate cases, 1000 data sets were automatically simulated using the fitted parameters with Gaussian error added whose standard deviation was taken to be the overall error of the fit.

2.7. Differential scanning calorimetry

DSC experiments were done using a Calorimetric Sciences, Inc. (Spanish Fork, UT) NanoDSC instrument. Sample concentrations for DSC studies were 156 μM (in strands). Scan rates of 1 °C min^{-1} were used in all cases. Buffer versus buffer baseline scans were determined and subtracted from denaturation scans prior to normalization and analysis [35]. Binding parameters were determined from DSC thermograms in the presence and absence of ligand using the theory provided by Brandts and Lin [36].

2.8. Isothermal titration calorimetry (ITC)

Calorimetric titration data were obtained using a Calorimetry Sciences Corporation (Spanish Fork, UT) CSC4200 isothermal microtitration calorimeter linked to a Gateway 2000 PC. The reference cell was filled with distilled water. The instrument was routinely calibrated using the neutralization of NaOH by HCl as a calibration reaction, where an enthalpy value of -13.63 kcal mol^{-1} at 20 °C has been accurately determined [37]. Both reagents are available as highly pure, standardized aqueous solutions from Aldrich Chemical Co. (St. Louis, MO). For instrument calibration, a 0.0995 M NaOH volumetric solution (cell volume = 1.00 mL) was titrated with serial 3-μL injections of aqueous 0.1036 M HCl solution. Data for up to 20 injections in a single run were accumulated and averaged for comparison with the known enthalpy value.

Binding enthalpies for the argininamide–aptamer were determined using the "model-free ITC" protocol in order to obtain multiple estimates of $\Delta H°$ and to avoid any possible fitting bias [38]. In this procedure, a large excess of argininamide was placed in the calorimeter cell and aliquots of aptamer are then titrated into the ligand solution following thermal equilibration. The high ligand concentration ensures that all added aptamer is effectively saturated after each serial addition. Integration of each titration peak and normalization for the moles of ligand added provides a direct and model-free estimate of the binding enthalpy, without recourse to any curve fitting or assumed binding model(s). Specifically, 10 μL aliquots of 0.2 mM aptamer stock solution were added to 1 mL of a 3 mM L-argininamide solution, usually making 20 injections with 5 min between injections to ensure equilibration. The titrate solution was stirred continuously at 50 rpm over the course of the experiment. Data were collected as heat released (μJ) in the exothermic reactions versus time (s). The heat of reaction ($\Delta H°$) was obtained by integration of the peak obtained after each injection. Heats of dilution for the aptamer were determined separately by injecting aptamer solution into the same reaction cell loaded with buffer alone. The dilution heats were subtracted from the ΔH value determined for titration into DNA to give a corrected value for the binding-induced enthalpy change. All titration series were repeated at least three times, and the averaged binding enthalpies ($\Delta H°$) were obtained after normalization and necessary correction for any heats of dilution.

2.9. Heat capacity change determination

The isobaric heat capacity (ΔC_p) accompanying the binding of L-argininamide (L-Arm) to the DNA aptamer 1OLD was performed using a MicroCal VP-ITC (Northampton, MA) isothermal titration calorimeter. Integrations were performed using the VPViewer software application and confirmed by integration in Origin 7.0. *Y*-axis (i.e., power) calibration was performed manually by both differential power calibration pulses to expose errors greater than 1% and chemically against the previously determined enthalpy for the binding of L-Arm to 1OLD. Samples were thermostatted and degassed prior to use using MicroCal's ThermoVac temperature-regulated degassing/equilibration unit.

Molar enthalpies ($\Delta H°$) were determined using the same "model-free" method previously described by subtraction of the raw heats of dilution from the experimental data. In these studies, 5.0 μL aliquots of a 0.2 mM aptamer buffered stock solution were added to 1.8 mL of a buffered 20.00 mM L-argininamide solution. Enthalpy determinations were determined over a range of temperatures with constant stirring and with a total of 10 injections per temperature. For each run, the loaded samples was pre-equilibrated and stirred for 1000 before the first injection for baseline equilibration. The time between injections was 200 s. The titrate solution was stirred continuously at 400 rpm over the course of the experiment. Data were collected as differential power (μcal min^{-1}) versus time (s).

2.10. Mfold calculations

All experimentally determined T_m and ΔH values were compared to those returned from the DNA folding algorithm *Mfold* [39]. The *Mfold* engine is available at http://www.bioinfo.rpi.edu/applications/mfold. The sequence of 1OLD was input and the ionic strength was set to 60 mM which mimics the solution conditions of the thermal denaturation experiments.

2.11. Binding studies

All CD detected binding isotherms were carried out at 20 °C in buffer A with a fixed amount of DNA aptamer [DNA] and variable L-Arm [*L*]. Titration data were extracted from whole CD spectra at 280 nm and the resulting binding isotherms were fit with Eqs. (2a)–(2d) [33] using GraphPad Prism 4.0. Eq. (1c) is the parent quadratic equation which is derived for a single site binding model and is composed of Eqs. (2a) and (2b). Eq. (2d) allows the direct application of the quadratic to circular dichroism data and is composed of Eqs. (2a)–(2c).

$$\alpha = \left\{-(K_{eq}*[L]) + (K_{eq}*[\mathrm{DNA}] + 1)\right\} \tag{2a}$$

$$\beta = \{(K_{eq}*[L]*[\mathrm{DNA}])\} \tag{2b}$$

$$\gamma = \left\{-\alpha - \sqrt{\frac{\alpha^2 - (4*K_{eq}*\beta)}{2*K_{eq}}}\right\} \tag{2c}$$

$$\mathrm{CD}_{observed}([L]) = \left\{\left(\frac{\gamma}{[\mathrm{DNA}]}\right)*((\mathrm{CD}_{bound} - \mathrm{CD}_{free}) + \mathrm{CD}_{free})\right\} \tag{2d}$$

In these equations, the fitted parameters are K_{eq} which is the equilibrium binding constant, CD_{bound} which is the CD detected molar ellipticity (θ) in units of millidegrees of the bound DNA, and CD_{free} which is the CD in millidegrees of the free DNA aptamer. The term [DNA] is the molar concentration of fixed DNA aptamer and [*L*] is the independent variable and is the molar concentration of ligand (i.e., L-argininamide) which ranges from 1×10^{-9} to 1×10^{-2} M. In these experiments [DNA] is 5.0×10^{-6} M. The dependent variable is $CD_{observed}$

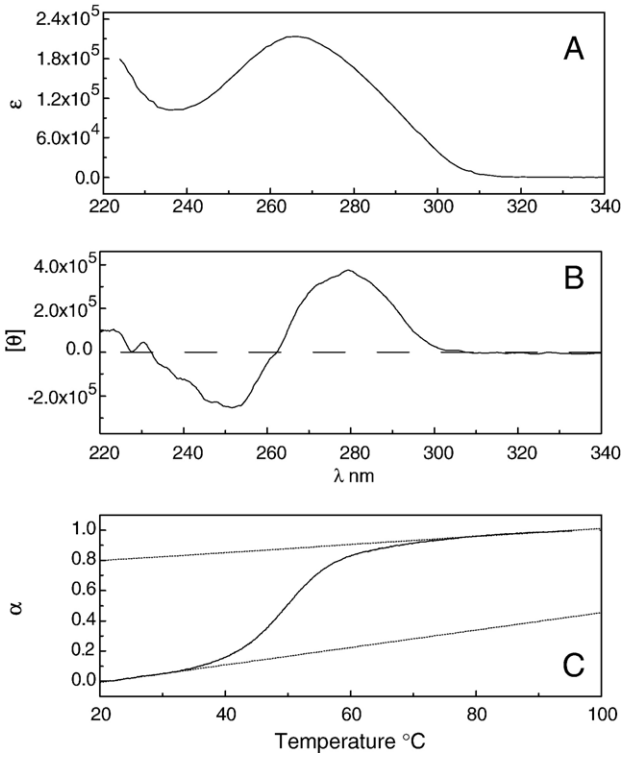

Fig. 2. Optical properties of the DNA aptamer 1OLD. (A) The ultraviolet (UV) spectrum of the aptamer with the molar extinction coefficient (ε) plotted versus wavelength. (B) The circular dichroism (CD) spectrum of the same aptamer. (C) The optically determined thermal denaturation of 1OLD with the absorbance at 260 nm (A_{260}) versus temperature (T) plotted. The curve through the raw data points in panel C is the best fit of the data by Eqs. (1a)–(1f). The dashed lines are the best linear fits to the pre- and post-transition baselines.

which is the measured CD signal in millidegrees obtained at 280 nm.

2.12. Molecular modeling

The NMR structure 1OLD.ent was used to create the starting model of the hairpin with L-argininamide removed. We performed molecular dynamics simulations separately on L-argininamide and the unbound DNA hairpin using the AMBER* force field within Macromodel and implicit solvation (GB/SA water approximation) for a production run of 1 ns (time-step of 1.5 fs, 300 K). A continuation of the production run for 10 ps was used to sample and average 10 snapshots that was subsequently minimized (1000 steps steepest descents followed by 5000 steps of conjugate gradient). The surface area calculations used Naccess 2.1.1.

3. Results

3.1. Optical melting studies

To examine the energetic basis of DNA aptamer molecular recognition and the role that ligand binding plays in stabilizing the folded state, a series of CD binding, UV-melting and microcalorimetry experiments were carried out. Fig. 2 shows selected spectral properties of DNA aptamer 1OLD in the absence of ligand (Table 1). 1OLD has an essentially featureless but typical DNA UV–absorption spectrum (Fig. 2A) with a maximum at 266 nm. Its CD spectrum (Fig. 2B) is characteristic of right-handed DNA [24,30]. The UV detected (at 260 nm) thermal denaturation of 1OLD in the absence of the ligand is shown in Fig. 2C. Melting curves such as that presented in Fig. 2C can be analyzed by several different methods to obtain estimates of the T_m, the unfolding enthalpy ($\Delta H°$) and the standard Gibbs free energy ($\Delta G°$). Each of these methods assumes a single two-state transition. Those methods include; (1) a direct fit of the A_{260} versus temperature (T) data by Eqs. (1a)–(1f); (2) conversion of the A_{260} data into fraction folded (α) versus T with subsequent conversion into a van't Hoff plot of $\ln K_T$ versus $1/T$ or; (3) analysis of the first derivative of melting curves displayed as $d\alpha/dT^{-1}$ versus $1/T$. In each case, some correction for sloping pre- and post-transition baselines is necessary. The spectrophotometric data (Fig. 2C) clearly exhibit sloping pre- and post-transition baselines, as indicated by the fitted straight lines. The results of a direct fit to the primary data by Eqs. (1a)–(1f) are presented as the curve through the data. Table 1 summarizes the T_m and ΔH values for the unfolding of 1OLD obtained using each of the different analytical methods. In each case, the experimental values are in excellent agreement with the values of T_m=49.6 °C and $\Delta H°$=51.2 kcal mol^{-1} predicted by the *Mfold* algorithm [39] for the stem–loop structure shown in Fig. 1A.

Table 1
Thermodynamic parameters for folding the DNA aptamer 1OLD

Method of analysis	Folding thermodynamic parameters [a]			
	T_m (°C)	$\Delta H°$ (kcal mol^{-1})	$\Delta G°$ [b] (kcal mol^{-1})	$T\Delta S°$ [b] (kcal mol^{-1})
Mfold [c]	49.6	−51.2	−2.0	−49.2
$\alpha(T)$ [d]	48.24 (0.14) [e]	−50.10 (0.24)	−2.85 (0.15)	−47.25 (0.28)
$d\alpha/dT$ [f]	48.58 (0.14)	−49.87 (1.10)	−2.92 (0.06)	−46.95 (1.10)
van't Hoff [g]	48.38 (0.15)	−49.76 (0.62)	−2.87 (0.06)	−47.06 (0.62)
Direct Fit [h]	48.56 (0.02)	−52.38 (0.23)	−3.08 (0.01)	−48.91 (0.23)
Monte Carlo [i]	48.36 (0.02)	−51.05 (0.23)	−2.94 (0.01)	−48.11 (0.23)
Monte Carlo [j] (ave. 3 experiments)	47.96 (0.55)	−50.31 (1.07)	−2.80 (0.07)	−47.51 (1.07)
DSC i (ave. 9 experiments)	50.2 (0.2)	−49.0 (2.1)	−3.3 (0.1)	−45.7 (3.6)

[a] Standard deviations are in parentheses.
[b] Parameters computed at a temperature (T) of 37 °C.
[c] Computed at a sodium concentration of 0.06 M and at 37 °C by the *mfold* algorithm.
[d] Fraction folded (α) versus temperature (T).
[e] Determined by differential scanning calorimetry (DSC).
[f] First derivative of the fraction folded (α) versus T plot.
[g] T_m and enthalpy ($\Delta H°$) determined by van't Hoff plot ($\ln K_{eq}$ versus $1/T$).
[h] The absorbance at 260 nm (A_{260}) versus T plot was fit directly by the equation:
[i] Monte Carlo results were obtained by fitting 1000 simulated data sets containing the same dependent values (T) for the raw data by the direct fit equation. The standard deviation of each raw data fit was used for generating random Gaussianly distributed error for each Monte Carlo simulation. T_m and $\Delta H°$ values obtained for each fit were then averaged and their standard deviations reported.
[j] Averaged results from Monte Carlo simulations of three independent melts of 1OLD from different synthetic batches.

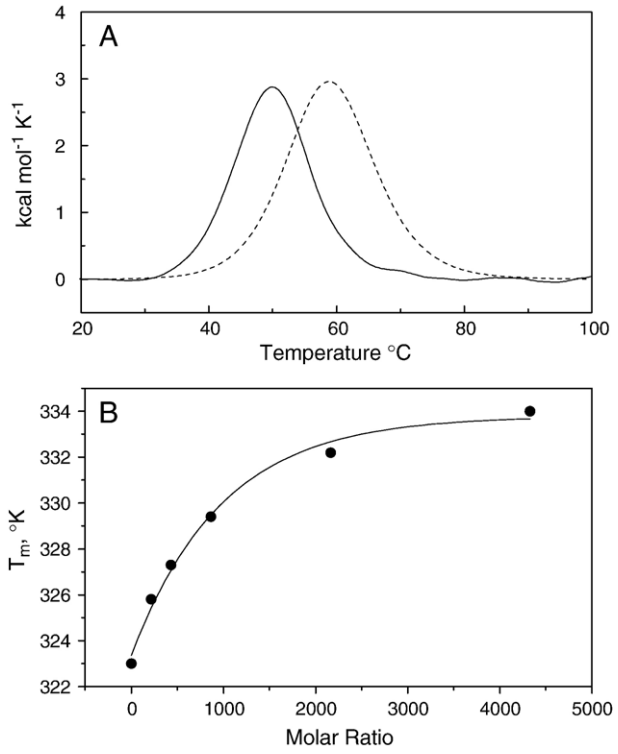

Fig. 3. Differential scanning calorimetry (DSC) detected binding of L-argininamide to 1OLD. (A) The DSC melt of the DNA aptamer 1OLD (156 μM strand concentration) in the absence (solid line) and presence (dashed line) of a saturating concentration (10 mM) of the ligand L-Arm. (B) The plot of the DSC detected T_m in the presence of increasing concentrations of L-Arm. T_m values were extracted from the raw DSC melts such as those shown in panel A.

3.2. Differential scanning calorimetry (DSC) melting studies

To further investigate the thermal denaturation of 1OLD, DSC experiments were carried in the absence and presence of L-Arm over a range of aptamer concentrations. Fig. 3A shows the denaturation thermogram of the aptamer. Table 1 also shows the results of independent replicate DSC experiments ([aptamer strand] = 100 μM) along with the optical melt results in the absence of the ligand L-Arm. The more direct DSC determined T_m and ΔH values compare well with those parameters obtained by optical methods (Table 1) and with the values computed by *Mfold*. The equivalence of the calorimetric and van't Hoff enthalpy values indicates that the unfolding of 1OLD is a simple two-state process, with no discernable intermediates.

Fig. 4A presents the effect of the aptamer strand concentration on the melting point (T_m) in the range of 0.16–69.3 μM in the absence of ligand. These results indicate that the observed T_m of 1OLD is independent of the aptamer strand concentration and that the denaturation reaction is a simple unimolecular process, as expected. Fig. 4B shows the effect of increasing KCl concentration on the T_m of the aptamer. A linear fit of the effect of ion concentration on the DSC measured T_m reveals that increasing salt concentration increases the T_m and hence the overall stability of the aptamer in the absence of any ligand (Fig. 4B). The slope of the fitted line is 9.06 ± 0.64 and the intercept is 335.60 ± 0.80 °C.

3.3. Binding studies

Complete characterization the binding thermodynamics in this system requires determination of the standard state binding free energy ($\Delta G°$), enthalpy ($\Delta H°$) and entropy ($\Delta S°$). Binding was studied by circular dichroism (Fig. 5), isothermal titration calorimetry (ITC) (Fig. 4) and by differential scanning calorimetry (Fig. 3).

The CD spectrum of the DNA aptamer (Fig. 5A; thin solid line) is strikingly different from the L-Arm–aptamer complex (Fig. 5A; thick solid line). Changes in the molar ellipticity at 280 nm with increasing concentrations of L-Arm define the ligand binding isotherm (Fig. 5B). An estimate of the binding equilibrium constant can be extracted from these data assuming a single independent binding site for the ligand (Table 2). A binding constant of 5998 ± 920 M^{-1} was determined, from which a binding free energy of −5.1 kcal mol^{-1} was calculated.

3.4. Isothermal titration calorimetry (ITC) studies

The binding enthalpy can be directly measured by "model-free" ITC experiments in which low concentrations of aptamer are added to a molar excess of ligand (e.g., 10 μL aliquots of 0.2 mM aptamer into 1 mL of a 3.0 mM L-Arm). In this manner all added aptamer is bound by the ligand and, thus, extraction of the enthalpy requires no application of any binding model to fit the data. Fig. 6A shows the raw data obtained from a single

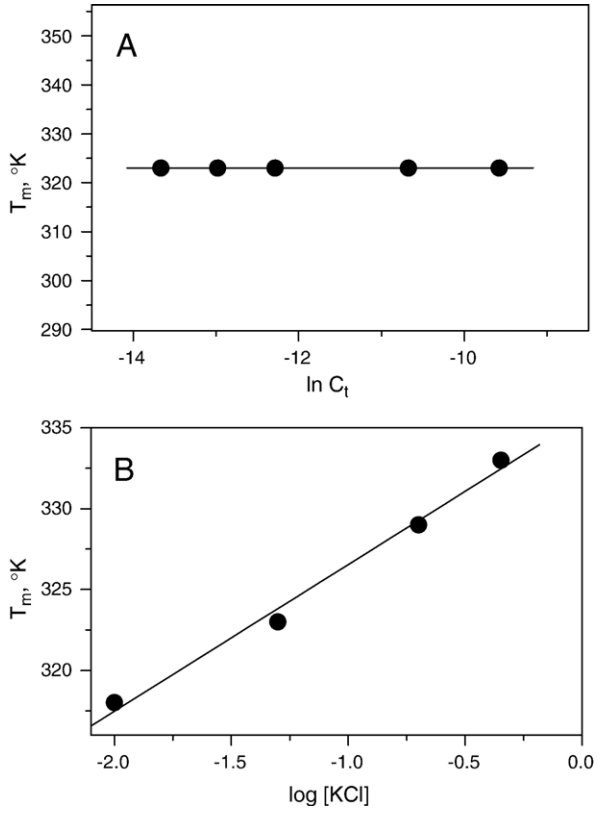

Fig. 4. Effect of strand and KCl concentration on the DSC detected thermal denaturation of 1OLD. (A) The effect of strand concentration on the T_m of 1OLD. (B) The effect of increasing [KCl] on the T_m of 1OLD. The line is the best linear fit through the data.

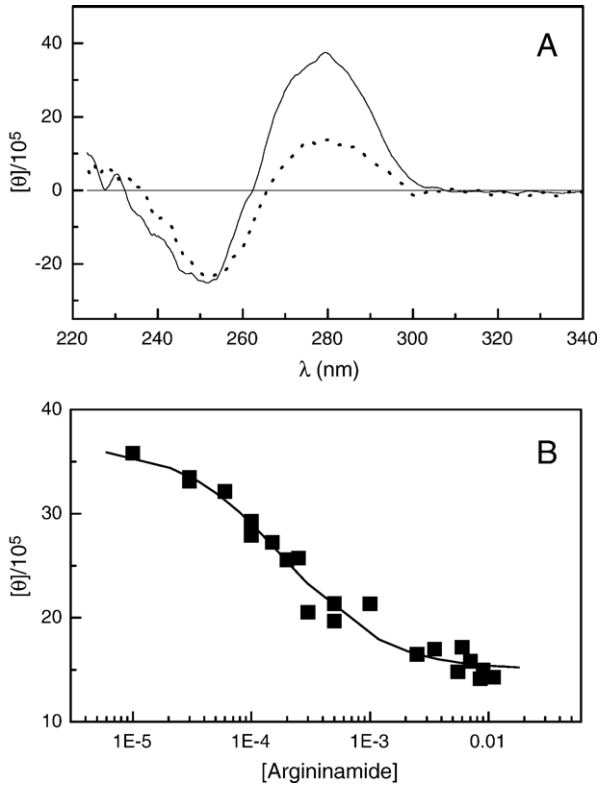

Fig. 5. Binding of L-argininamide to 1OLD detected by circular dichroism. (A) CD spectra of the aptamer alone at 2.3 μM strand concentration (thin solid line) and 2.3 μM aptamer+10 mM L-argininamide (thick solid line). (B) Binding isotherm of the interaction of L-argininamide with the aptamer. A fixed concentration (2.38 μM) of aptamer was titrated with L-argininamide while monitoring the molar ellipticity at 282 nm. Primary data are show as solid symbols. The line is the best fit of the data to Eqs. (1a)–(1f), yielding a binding constant $K=5998\ (\pm 920)\ M^{-1}$, $[\Theta]_0=3.65\ (\pm 0.1)\times 10^5$, and $[\Theta]_b=1.50\ (\pm 0.1)\times 10^5$. $[\Theta]_0$ and $[\Theta]_b$ are the molar ellipticity of the free aptamer and the saturated complex, respectively.

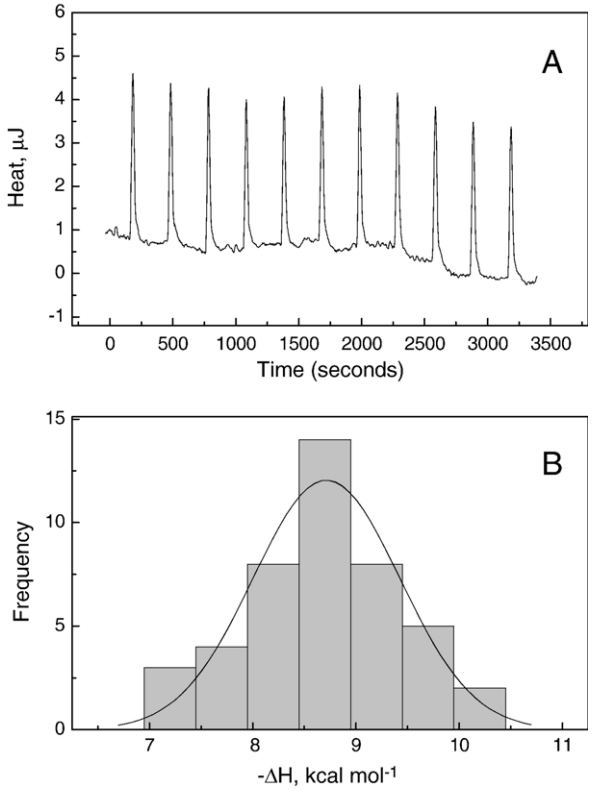

Fig. 6. Results from isothermal titration calorimetric (ITC) experiments. (A) Primary data from the addition of 10 μL aliquots of 0.2 mM aptamer stock solution to 1 mL of a 3 mM L-argininamide solution. (B) Distribution of enthalpy values determined from four separate experiments. A Gaussian fit to the distribution is shown by the solid line, yielding $\Delta H_{cal}=-8.7\ (\pm 0.8)$ kcal mol^{-}1.

model free ITC run with 11 injections at 25 °C. Fig. 6B is the distribution of molar enthalpies obtained from multiple ITC runs such as those presented in Fig. 6A. The molar enthalpy is simply the concentration corrected area under the peaks in Fig. 4A which are the results from individual injections. After correction for the heat of dilution, the overall enthalpy of binding was found to be -8.7 kcal mol^{-1}. When combined with the free energy of binding from CD titrations, the entropic contribution to binding can be computed from rearrangement of the Gibbs free energy relationship, $-T\Delta S^\circ=\Delta G^\circ-\Delta H^\circ=+3.6$ kcal mol^{-1} (Table 2).

Fig. 3B presents results of DSC experiments in the absence (Fig. 3A, solid line) and presence (Fig. 3A, dashed line) of the L-Arm ligand. The melting point of the L-Arm-bound DNA aptamer 1OLD is higher than for the unbound aptamer, and is therefore a more energetically stable structure. A similar melting temperature increase is observed in UV-absorbance data and CD melting curves. Fig. 3B shows the effect of increasing [L-Arm] on the observed T_m. From these data it is possible to extract the free energy of binding as well as the enthalpy of binding, yielding the values shown in Table 2. The results agree with those results obtained by combined CD and ITC.

Table 2
Thermodynamics of L-Arm binding to DNA aptamer 1OLD

Method	K_{eq} (M^{-1})	ΔG° (kcal mol^{-1})	ΔH° (kcal mol^{-1})	$-T\Delta S^\circ$ (kcal mol^{-1})
DSC	6034	−5.10	−9.2	+4.1
ITC	Not done	Not done	−8.7±0.8	+3.6
CD	5998	−5.06	Not done	+3.6

3.5. Heat capacity (ΔC_p) results

The temperature dependence of the enthalpy was studied by ITC at four temperatures over the range of 15–40 °C to determine the molar heat capacity, $\Delta C_p=(\delta\Delta H/\delta T)$. A value of -116 ± 29 cal mol^{-1} K^{-1} was determined.

3.6. Calculation of the change in solvent accessible surface area upon complex formation

The model of the unligated form of the 24-mer DNA derived from the molecular dynamics is relatively consistent with the NMR structure of the 24-mer DNA [2]. Lin and Patel state [2] that the A7·T18 and A6·T19 base pairs are not observed in the unligated form but are stabilized (and observed) upon argininamide binding. Our 24-mer DNA model shows that the

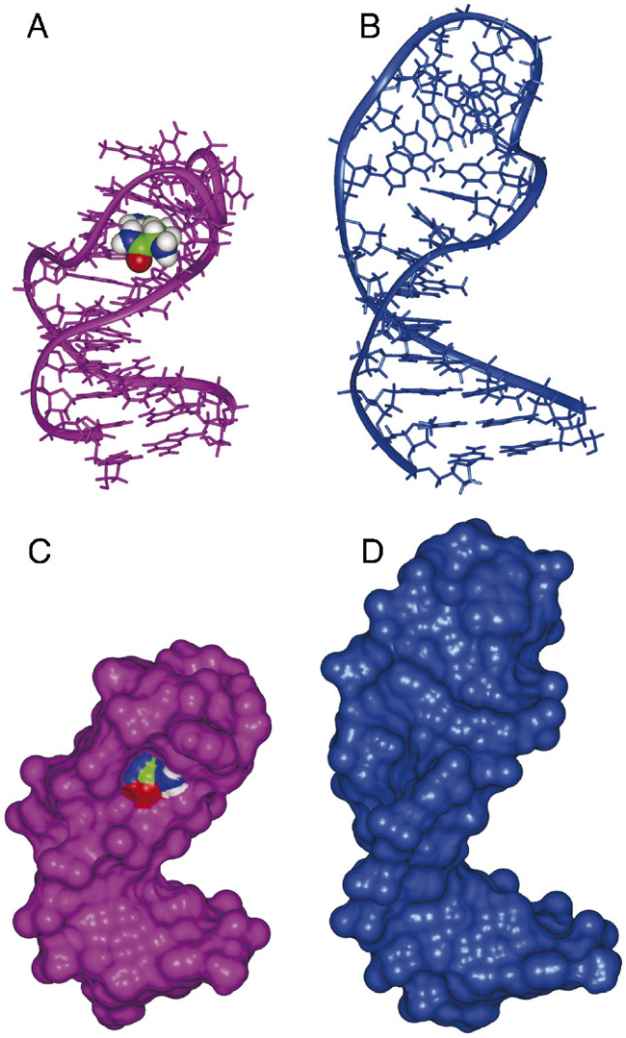

Fig. 7. The L-argininamide bound and unbound form of 1OLD have significantly different shapes. (A) NMR structure 1OLD with L-argininamide rendered as CPK with atom colors. (B) Molecular model of the unbound form of 1OLD. (C) 1OLD with the Connelly surface colored in purple for DNA and by atom colors of L-argininamide. (D) Connelly surface of the unbound form of 1OLD. (For interpretation of the references to colour in this figure legend, the reader is referred to the web version of this article.)

A7·T18 basepair is not stable in the simulation. Fig. 7 shows models derived from published NMR studies and our molecular dynamics simulations on the unligated hairpin. Changes in solvent accessible surface areas upon complex formation were calculated from these structures as the differences between the L-Arm–aptamer complex and free reactants, L-Arm and the DNA hairpin. We found a net change in nonpolar solvent accessible surface area of -450.9 Å^2, and a change in polar solvent accessible surface area of -588.3 Å^2.

4. Discussion

The results presented here provide, for the first time, a complete thermodynamic profile for the adaptive recognition of a ligand by its DNA aptamer. The binding of L-argininamide to its DNA aptamer is highly selective, but is energetically weak, with a binding free energy of only -5.1 kcal mol^{-1}. The modest binding free energy results from opposing enthalpic and entropic contributions of $\Delta H^\circ = -8.7$ kcal mol^{-1} and $-T\Delta S^\circ = +3.6$ kcal mol^{-1}. The unfavorable entropy results from the ordering of the nucleic acid as it folds from a hairpin structure with a disordered loop region into a form with a well-defined binding pocket that engulfs L-argininamide (Fig. 1). One key lesson to emerge from our studies is that high selectivity in binding need not require high affinity.

Fig. 7 provides a dramatic visualization of the conformational transition that is coupled to L-Arm binding. The dynamic loop structure in the unligated aptamer almost completely engulfs the ligand, leading to a highly ordered binding pocket stabilized by the molecular interactions diagrammed in Fig. 1. The nucleic acid is greatly compacted upon folding around the ligand. The radius of gyration decreases from 1.583×10^{-7} cm in the unligated aptamer to 1.293×10^{-7} cm in the ligated form, a decrease of nearly 20%.

A comparison of the L-argininamide–aptamer binding thermodynamics with other small molecule–DNA binding interactions (Fig. 8) reveals an interesting trend. The bind of the groove binder Hoechst 33258 to DNA is entropically driven, with an unfavorable positive enthalpy [40]. For such groove binding, there is little perturbation of the DNA structure, with the ligand fitting into the minor groove in essentially a "lock-and-key" manner. Daunomycin binds to DNA by a mixed binding mode, with intercalation of its anthraquinone ring, but with groove binding of its daunosamine moiety [41]. As an intercalator, Daunomycin has one of the lowest observed unwinding angles of only 11° [42]. Its binding is driven by a large, favorable enthalpy and is opposed by only a slight unfavorable enthalpy [38]. Ethidium is perhaps the classic intercalator, with an unwinding angle of 26° [42]. Its binding to DNA is weaker than Daunomycin, and its binding is opposed by a larger unfavorable entropy compared to Daunomycin [38]. Intercalators may be thought of as binding by an "induced fit" binding mode, and their unfavorable entropy of binding may correlate with the extent to which they must distort the DNA to form their required intercalation site [43]. For comparison, data for the L-argininamide–aptamer binding thermodynamics are

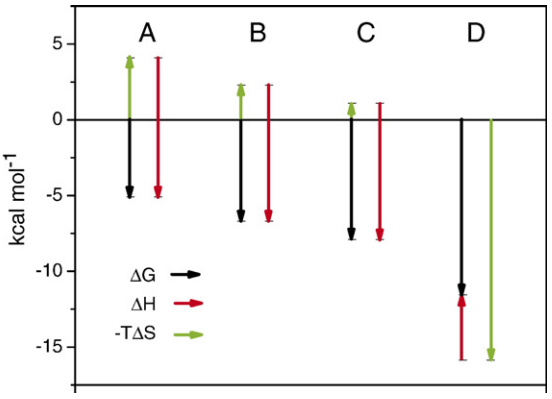

Fig. 8. Comparison of the thermodynamic profiles for ligand–nucleic acid binding reactions. (A) L-argininamide binding to its aptamer. (B) Intercalation of ethidium bromide into calf-thymus DNA. (C). Intercalation of daunorubicin into calf-thymus DNA. (D) Binding of Hoechst 33258 to d(CGCAAATTTGCG)$_2$.

shown in Fig. 8, to emphasize the even more extreme partitioning of entropic and enthalpic contributions of the binding free energy, correlating with a more extreme reordering of the nucleic acid structure compared to the other DNA binders.

Our data for the denaturation of the unligated aptamer sequence are consistent with the hairpin structure shown in Fig. 1. *Mfold* calculations for that secondary structure predict T_m and enthalpy values that are in excellent agreement with the experimentally observed values. The A7·T18 and A6·T19 base pairs were reported to be stabilized upon complex formation, and only then could their thymine imino protons be observed by NMR. Our data suggest, however, that those base pairs contribute to the stability of the unligated structure. Molecular dynamics simulations, however, indicate that while A6·T19 is stable within the stem structure in the absence of L-argininamide, A7·T18 is not, and the base pair is disrupted over the course of the trajectory.

Molecular dynamics simulations on the ligated and unligated structures indicate that upon complex formation there is a reduction of −450.9 Å^2 in nonpolar solvent accessible surface area, and a reduction of −588.3 Å^2 in polar solvent accessible surface area. These values may be used to estimate the heat capacity change that accompanies the binding of L-argininamide using the empirical relationship derived by Spolar and Record [23]:

$$\Delta C_p = 0.32(-588.3) - 0.14(-450.9) = -125 \text{ cal mol}^{-1}\text{ K}^{-1}$$

The calculated value is in excellent agreement with the experimentally determined value of −116±29 cal mol^{-1} K^{-1}. The heat capacity change provides a means for linking structural and energetic data, and the close agreement between the predicted and actual value suggests that the structures illustrated in Fig. 7 are the plausible starting and end points of the conformational transition that occurs in the aptamer sequence upon complex formation. An alternate explanation for the negative heat capacity change is that it arises from the coupling of binding to a temperature-dependent conformational transition in the nucleic acid [41]. We cannot definitively distinguish between models, although the removal of solvent accessible surface area seems to quantitatively account for our data.

We caution that our thermodynamic data refer to the overall process of complex formation, and can not define the reaction pathway. At least two pathways are possible that define the branches of a thermodynamic cycle:

1. L-Arg + Aptamer ↔ L-Arg·Aptamer ↔ L-Arg·Aptamer*
2. L-Arg + Aptamer ↔ L-Arg + Aptamer* ↔ L-Arg·Aptamer*

where "Aptamer*" represents the collapsed conformational form containing a fully formed (but unoccupied) binding pocket. In pathway 2, the aptamer conformational transition precedes binding, whereas in pathway 1 it occurs after transient complex formation. Resolution of these pathways is a kinetic problem for which we currently have no information or data. Interestingly, NMR studies by the Wemmer laboratory using a closely related aptamer sequence [3] provided suggestive evidence for complicated binding kinetics that perhaps involved a slow interconversion of two DNA conformations prior to binding. Such behavior would support pathway 2 as the kinetically favored reaction mechanism.

In summary, our data provide one of the first thermodynamic characterizations of adaptive recognition in a DNA aptamer. Our data show that high selectivity need not require high affinity, and indeed that selective induced-fit binding may require compensating enthalpic and entropic terms.

5. Postscript

One of us (JBC) had the privilege of working with Julian Sturtevant on several occasions, and would like to offer some fond recollections. While I was a postdoc with Don Crothers at Yale, I never actually collaborated with Julian, although I often intercalated myself into the afternoon teatime he held in his lab. Conversation at these events was eclectic, but often as not included a political rant against the Reagan administration. In 1986, after getting my first faculty position, I asked Julian for help with calorimetry, and he kindly agreed to host me and to mentor me in the method. I spent several weeks in Julian's laboratory measuring the enthalpy of the B to Z transition in DNA. The experience was memorable on many counts. First, I was there at World Series time, and Julian had arranged housing for me in the Yale Divinity School. That Divine connection did not help my beloved Red Sox. That was the year of the infamous and heartbreaking Bill Buckner error which denied them the championship. I came to work after that deeply depressed, but I think that Julian was a Yankee fan, so he didn't care that much. Second, I learned how much calorimetry costs, literally. While preparing samples for our DSC runs, I asked Julian how much was needed, and he answered immediately "more". As a result, one DSC experiment had $1000 worth of poly (dGdC) in the sample cell, an amount that represented 1/12 of the supply budget of my modest NIH grant. The data looked great! I had planned carefully, and intended to reclaim the sample after the DSC run for use in other spectroscopic experiments. I could have worked for months with that large amount of material. After the run, I momentarily turned away, and when I looked back, to my horror, Julian was aspirating my precious sample (and supply budget) down the drain while cleaning the DSC! I fought back tears, calmed the knots in my stomach, and carried on. I never told Julian that he had rinsed away a good part of my supply money for the year. It was all worthwhile when the experiments were done, the data analyzed, and Julian and I were discussing the results. I showed Julian numerous published papers that had attempted to determine the enthalpy of the B to Z transition by spectroscopic means using van't Hoff analysis. The results were confusing and contradictory, and the weak consensus was that the B to Z transition was entirely entropically driven, with zero enthalpy. Julian thumbed through the papers, grunting occasionally, smiling on others. He finally tossed them on the table, tapped our thermogram with this finger, and said, "I don't care what these folks say, this, by God, is the enthalpy". Such confidence

was comforting! I then tried to interest Julian in a hot-off-the-press *Science* article from some prominent investigators that purported to calculate the entropy of the B to Z transition from "first principles". They had calculated an entropy that was completely opposite in sign from what we had just measured! Julian scanned the article with increasing visible scorn, tossed it down, and said, "I guess these theoreticians don't know how to calculate entropies yet, huh?" One final memory is of Julian at the 1993 Gibbs Conference on Biological Thermodynamics. Julian was a keynote speaker, and discussed his recent data on protein–DNA interactions that were perceived to be "anomalous" because measured heat capacity changes did not correlate with calculated changes in solvent accessible surface areas. Julian presented his data, pointed out the "anomaly", and finished his talk by saying, "What I conclude from this is that we should spend more time improving the accuracy of measured heat capacity changes, and less time speculating what those values mean." In the current climate of hypothesis-driven research, "rational" drug discovery, and the mania for academic scientists to start biotech companies based on the often mundane finding of the month, Julian's attitude would have little currency. That is to the detriment of our enterprise. It is an attitude that will be greatly missed.

Acknowledgements

Supported by Grant CA35635 from the National Cancer Institute (to JBC), and by Cottrell College Science Award CC5939 (to GRB) from the Research Corporation.

References

[1] K. Harada, A.D. Frankel, Identification of two novel arginine binding DNAs, EMBO J. 14 (1995) 5798–5811.
[2] C.H. Lin, D.J. Patel, Encapsulating an amino acid in a DNA fold, Nat. Struct. Biol. 3 (1996) 1046–1050.
[3] S.A. Robertson, K. Harada, A.D. Frankel, D.E. Wemmer, Structure determination and binding kinetics of a DNA aptamer–argininamide complex, Biochemistry 39 (2000) 946–954.
[4] C.H. Lin, W. Wang, R.A. Jones, D.J. Patel, Formation of an amino-acid-binding pocket through the adaptive zippering-up of a large DNA hairpin loop, Chem. Biol. 5 (1998) 555–572.
[5] C.H. Lin, D.J. Patel, Structural basis of DNA folding and recognition in an AMP–DNA aptamer complex: distinct architectures but common recognition motifs for DNA and RNA aptamers complexed to AMP, Chem. Biol. 4 (1997) 817–832.
[6] V.M. Marathias, P.H. Bolton, Structures of the potassium-saturated, 2:1, and intermediate, 1:1, forms of a quadruplex DNA, Nucleic Acids Res. 28 (2000) 1969–1977.
[7] V.M. Marathias, K.Y. Wang, S. Kumar, T.Q. Pham, S. Swaminathan, P.H. Bolton, Determination of the number and location of the manganese binding sites of DNA quadruplexes in solution by EPR and NMR in the presence and absence of thrombin, J. Mol. Biol. 260 (1996) 378–394.
[8] Y. Li, C.R. Geyer, D. Sen, Recognition of anionic porphyrins by DNA aptamers, Biochemistry 35 (1996) 6911–6922.
[9] C. Boiziau, E. Dausse, L. Yurchenko, J.J. Toulme', DNA aptamers selected against the HIV-1 *trans*-activation-responsive RNA element form RNA–DNA kissing complexes, J. Biol. Chem. 274 (1999) 12730–12737.
[10] A.D. Ellington, J.W. Szostak, Selection in vitro of single-stranded DNA molecules that fold into specific ligand-binding structures, Nature 355 (1992) 850–852.
[11] G.F. Joyce, In vitro evolution of nucleic acids, Curr. Opin. Struct. Biol. 4 (1994) 331–336.
[12] C. Tuerk, L. Gold, Systematic evolution of ligands by exponential enrichment: RNA ligands to bacteriophage T_4 DNA polymerase, Science 249 (1990) 505–510.
[13] E.N. Brody, L. Gold, Aptamers as therapeutic and diagnostic agents, J. Biotechnol. 74 (2000) 5–13.
[14] L. Cerchia, J. Hamm, D. Libri, B. Tavitian, V. de Franciscis, Nucleic acid aptamers in cancer medicine, FEBS Lett. 528 (2002) 12–16.
[15] S.L. Clark, V.T. Remcho, Aptamers as analytical reagents, Electrophoresis 23 (2002) 1335–1340.
[16] V. Dapic, V. Abdomerovic, R. Marrington, J. Peberdy, A. Rodger, J.O. Trent, P.J. Bates, Biophysical and biological properties of quadruplex oligodeoxyribonucleotides, Nucleic Acids Res. 31 (2003) 2097–2107.
[17] J. Feigon, T. Dieckmann, F.W. Smith, Aptamer structures from A to Z, Chem. Biol. 3 (1996) 611–617.
[18] T. Hermann, D.J. Patel, Adaptive recognition by nucleic acid aptamers, Science 287 (2000) 820–825.
[19] B.I. Kankia, L.A. Marky, Folding of the thrombin aptamer into a G-quadruplex with Sr(2+): stability, heat and hydration, J. Am. Chem. Soc. 123 (2001) 10799–10804.
[20] I. Smirnov, R.H. Shafer, Effect of loop sequence and size on DNA aptamer stability, Biochemistry 39 (2000) 1462–1468.
[21] K. Sumikura, K. Yano, K. Ikebukuro, I. Karube, Thrombin-binding properties of thrombin aptamer derivatives, Nucleic Acids Symp. Ser. 37 (1997) 257–258.
[22] A.S. Brodsky, J.R. Williamson, Solution structure of the HIV-2 TAR–argininamide complex, J. Mol. Biol. 267 (1997) 624–629.
[23] R.S. Spolar, M.T. Record Jr., Coupling of local folding to site-specific binding of proteins to DNA, Science 263 (1994) 777–784.
[24] J.B. Chaires, Dissecting the free energy of drug binding to DNA, Anti-Cancer Drug Des. 11 (1996) 569–580.
[25] J.B. Chaires, Drug–DNA interactions, Curr. Opin. Struct. Biol. 8 (1998) 314–320.
[26] S.P. Edgcomb, K.P. Murphy, Structural energetics of protein folding and binding, Curr. Opin. Struct. Biol. 11 (2000) 62–66.
[27] S.J. Hughes, J.A. Tanner, A.D. Hindley, A.D. Miller, I.R. Gould, Functional asymmetry in the lysyl–tRNA synthetase explored by molecular dynamics, free energy calculations and experiment, BMC Struct. Biol. 3 (2003) 5–25.
[28] J.J. Boniface, Z. Reich, D.S. Lyons, M.M. Davis, Thermodynamics of T cell receptor binding to peptide–MHC: evidence for a general mechanism of molecular scanning, Proc. Natl. Acad. Sci. U. S. A. 96 (1999) 11446–11451.
[29] P.N. Borer, Handbook of Biochemistry and Molecular Biology, Nucleic Acids, CRC Press, Boca Raton, 1975.
[30] G.R. Bishop, J.B. Chaires, Characterization of DNA structures by circular dichroism, Curr. Prot. Nucl. Acid Chem. 7 (2002) 7.11.1–7.11.8.
[31] J.D. Puglisi, I. Tinoco, Absorbance melting curves of RNA, Methods Enzymol. 180 (1989) 304–325.
[32] G.E. Plum, Optical methods, Curr. Prot. Nucl. Acid Chem. 7 (2000) 7.3.1–7.3.17.
[33] X. Qu, J.B. Chaires, Analysis of drug–DNA binding data, Methods Enzymol. 321 (2000) 353–369.
[34] J.J. Correia, J.B. Chaires, Analysis of drug–DNA binding isotherms: a Monte Carlo approach, Methods Enzymol. 240 (1994) 593–614.
[35] D.S. Pilch, Calorimetry of nucleic acids, Curr. Prot. Nucl. Acid Chem. 7 (2000) 7.4.1–7.4.9.
[36] J.F. Brandts, L.N. Lin, Study of strong to ultralight protein interactions using differential scanning calorimetry, Biochemistry 29 (1990) 6927–6940.
[37] I. Granth, ACTA Chem. Scand. 24 (1970) 1067.
[38] J. Ren, T.C. Jenkins, J.B. Chaires, Energetics of DNA intercalation reactions, Biochemistry 39 (2000) 8439–8447.
[39] M. Zuker, *Mfold* web server for nucleic acid folding and hybridization prediction, Nucleic Acids Res. 31 (2003) 3406–3415.
[40] I. Haq, J.E. Ladbury, B.Z. Chodhry, T.C. Jenkins, J.B. Chaires, Specific binding of Hoechst 33258 to the $d(CGCAAATTTGCG)_2$ duplex: calorimetric and spectroscopic studies, J. Mol. Biol. 271 (1997) 244–257.

[41] J.B. Chaires, D. Satyanarayana, D. Suh, I. Fokt, T. Przewloka, W. Priebe, Parsing the free energy of anthracycline antibiotic binding to DNA, Biochemistry 35 (1996) 2047–2053.
[42] V.A. Bloomfield, D.M. Crothers, I. Tinoco, Nucleic Acids: Structures, Properties, and Functions, University Science Books, Sausalito, 2000.
[43] M.R. Eftink, R.L. Biltonen, Enthalpy–entropy compensation and heat capacity changes for protein–ligand interactions: general thermodynamic models and data for the binding of nucleotides to ribonuclease A, Biochemistry 22 (1983) 3884–3896.